Phase diagram and critical behavior of the adsorption system O/Ru(001): Comparison with lattice-gas models

P. Piercy
Department of Physics, University of Ottawa, Ottawa, Ontario, Canada K1N 6N5

K. De'Bell*
Department of Physics, Memorial University, St. John's, Newfoundland, Canada

H. Pfnür
Fakultät für Physik E20, Technische Universität München, D-8046 Garching, Federal Republic of Germany and Institut für Festkörperphysik, Universität Hannover, D-3000 Hannover 1, Federal Republic of Germany
(Received 1 July 1991)

The chemisorption of oxygen on the Ru(001) surface shows ordered $p(2\times2)$ and $p(1\times2)$ phases at coverages of $\frac{1}{4}$ and $\frac{1}{2}$ monolayer, respectively, that are observed to undergo apparently continuous transitions to a disordered state upon heating. We present here details of the experimental determination of the O/Ru phase diagram, lattice-gas models that describe it, and some (but not all) of the observed critical behavior. Monte Carlo simulations based on a phenomenological Hamiltonian describing pairwise interactions between adatoms are used to calculate the phase boundaries and (effective) critical exponents. Restricting adsorption of oxygen atoms to the triangular lattice of the hcp-type hollow sites as seen experimentally, repulsive first- and second-nearest-neighbor interactions are sufficient to describe the observed phase diagram at coverages $\Theta<0.4$ and the four-state Pott's-class critical exponents at $\Theta=\frac{1}{4}$, but fail to describe the higher coverage region. This model is then generalized to allow oxygen adsorption on both hcp- and fcc-type hollow sites, with a difference in binding energy of 0.52 eV between the two types of sites. At higher coverages, repulsive interactions within the adsorbate lead to a spillover of up to 12% of adatoms onto the sites of higher energy, markedly reducing the transition temperature at $\Theta=\frac{1}{2}$, in agreement with the experimental results on O/Ru(001). However, effective critical exponents computed for this model are near four-state Pott's values at $\Theta=\frac{1}{2}$, in contrast to the experimental data and suggestive of crossover behavior involving (2×2)-honeycomb and $p(2\times1)$ ground states.

I. INTRODUCTION

Structural phase transitions at surfaces have received considerable study over the past decade.[1] Order-disorder phenomena in chemisorbed, submonolayer systems have provided unique realizations of two-dimensional (2D) critical behavior, and are amenable to interpretation in terms of lattice-gas models.[2] In such models, effective interatomic interactions, both within the adsorbate and between the adsorbate and underlying substrate, provide an at least phenomenological explanation for the observed phase diagrams. (Microscopic calculations, based on the embedded-atom method, have also been used to derive these parameters, particularly for hydrogen adsorption.[3]) Using low-energy-electron-diffraction (LEED) methods, scaling behavior at continuous, structural transitions at surfaces has also been observed for a variety of systems.[4] In this paper, order-disorder transitions in the submonolayer adsorption of oxygen on the ruthenium(001) surface are studied. The phase diagram and critical exponents, as measured by LEED (Refs. 5–7), are discussed using the lattice-gas models[8–10] presented here, which also underline the differences between the ordering of atomic oxygen on the Ru(001) and Ni(111) surfaces.[11]

The structure of the O/Ru(001) system has been previously investigated using a variety of surface techniques.[12–18] The adsorption of oxygen is dissociative on this surface at and above room temperature,[13] with the binding energy of the adsorbed oxygen atom determined from thermal desorption measurements to be about 6.3 eV at a coverage of $\frac{1}{4}$, decreasing by about 1 eV at a saturation coverage of $\frac{1}{2}$.[12] (The coverage is defined as the number of adatoms per surface ruthenium atom.) The only LEED superstructure seen is (2×2), with maximum intensity observed at coverages of $\frac{1}{4}$ and $\frac{1}{2}$.[12] The identification of the saturation coverage with $\frac{1}{2}$ is supported by high-resolution electron-energy-loss measurements[15] and LEED observations on a stepped Ru(001) surface,[16] which suggest three domains of a $p(2\times1)$ structure at this coverage. This coverage assignment is also consistent with a room-temperature comparison of x-ray photoemission spectroscopy (XPS) O 1s intensities for a saturated oxygen layer with that of a $(\sqrt{3}\times\sqrt{3})R30°$ ordered CO structure on the same surface. Furthermore, recent LEED I-V analyses[19,20] of the ordered structures confirm $p(2\times1)$ ordering at saturation coverage of $\frac{1}{2}$, and a $p(2\times2)$ structure at coverage $\Theta=\frac{1}{4}$. At the lower coverage, oxygen adsorption is determined to occur at hcp-type threefold hollow sites on the Ru(001) surface, which is slightly reconstructed.[19] At

saturation coverage, oxygen adsorbs close to the hcp-type hollow sites, and the surface is again reconstructed, involving a buckling of the first two substrate layers and a pairing of ruthenium atoms parallel to the rows.[20]

The measurement of the phase diagram of the O/Ru(001) system,[5] as described in Sec. II, shows peak order-disorder transition temperatures of 754 and 555 K, occurring at coverages $\Theta=\frac{1}{4}$ and $\frac{1}{2}$, respectively. Critical exponents have also been measured for the apparently continuous transitions occurring at these two coverages, from LEED spot profile and intensity measurements made as a function of temperature, as previously described.[6,7] The $p(2\times2)$ structure at $\Theta=\frac{1}{4}$ disorders with observed critical exponents of the four-state Pott's universality class.[6] This is in agreement with Landau theory,[21] although ignoring the second Landau rule. At $\Theta=\frac{1}{2}$, an apparently continuous order-disorder transition and effective critical exponents were also observed,[7] although Landau theory predicts a first-order transition from the $p(2\times1)$ structure.

A structural study of the high-temperature, disordered phase has been completed recently by Pfnür, Lindroos, and Menzel,[22] analyzing very-low-energy electron-diffraction (VLEED) data using full dynamical LEED calculations. They find oxygen adsorption restricted to the hcp-type hollow site at coverages $\Theta=\frac{1}{4}$ and $\frac{1}{2}$ in the disordered phase as well. (The possibility of up to 20% of oxygen atoms residing on the fcc hollow site cannot be ruled out, however.) This result suggests that the adsorption phenomena observed in the O/Ru(001) system may be realistically modeled using lattice-gas models. In Sec. III we attempt to explain both the observed phase diagram and critical phenomena in this way.

II. EXPERIMENTAL

The LEED measurements were carried out in an UHV chamber at a base pressure of 2×10^{-11} mbar, as described recently.[6] LEED spot intensities and profiles were measured using a four-grid LEED system equipped with a Faraday cup whose movement was computer controlled. Measurements of the integrated spot intensities were made with a Faraday cup aperature subtending 3.4° in polar angle, while diffraction spot profiles and peak intensities were measured using a smaller cup aperature subtending 0.5°, and the incident beam current was less than 100 nA. The ruthenium crystal of 99.99% purity was cut and polished within 0.2° of the (001) plane. By liquid-nitrogen cooling and resistive heating through mounting wires spot welded to the back of the sample, temperature regulation to within 0.1K and programmed temperature ramping was possible. The relative relationship between coverage and dose was determined from O *KLL* Auger intensities measured by Maier,[23] and an absolute calibration made by taking the coverage to be exactly $\frac{1}{4}$ at the dose which gave the lower-coverage maximum in the order-disorder transition temperature.[6]

To determine the order-disorder phase boundary, the integrated LEED intensity of a $\frac{1}{2}$-order spot was measured as temperature was scanned, for fixed coverages. The phase-transition temperature was determined from the inflection point in these scans, a procedure that is physically justified by its correspondence with the heat-capacity maximum.[24] The phase boundary shown in Fig. 1 displays a sharp peak at $\Theta=\frac{1}{4}$ and a lower peak at $\frac{1}{2}$ coverage. Comparing measurements made ramping both up and down at maximum speeds of 4 K/s, no hysteresis or irreversibility could be detected, at temperatures above about 300 K. At lower temperatures, slow, electron-beam-induced degradation of the LEED spot intensity prevented accurate measurements, although the apparent damage disappeared on reheating. Measurements of the peak spot intensity, made with the small-aperature Faraday cup,[6,7] give transition temperatures in agreement with those determined from the integrated intensities, to within experimental error. Measurements of the diffraction spot width showed that no observable broadening occurred at accessible temperatures (i.e., above 300 K) and coverages within the ordered regions of the phase diagram, indicating an apparent absence of island formation (two-phase coexistence). The diffraction spots only broaden as the order-disorder transition boundary is crossed. We thus observe a single-phase $p(2\times2)$ structure near $\Theta=\frac{1}{4}$ which must undergo a transition to a single-phase $p(2\times1)$ structure at higher coverages. Equivalent data was obtained measuring different superstructure diffraction beams.

Note that the possible existence of a low-temperature island phase below about 300 K cannot be ruled out by our data. In fact, small clusters of oxygen atoms in the $p(2\times2)$ structure were observed recently at room temperature by a scanning tunnel microscope (STM) at coverages around 0.1 by Günther and Behm.[25]

The phase diagram described above for the O/Ru(001) system shows important differences in comparison with the O/Ni(111) phase diagram measured by Park *et al.*[11] While both systems show $p(2\times2)$ phases at coverages near $\frac{1}{4}$, and O/Ni system develops a $p(2\times2)$ antiphase domain phase and then a $(\sqrt{3}\times\sqrt{3})R30°$ phase as cover-

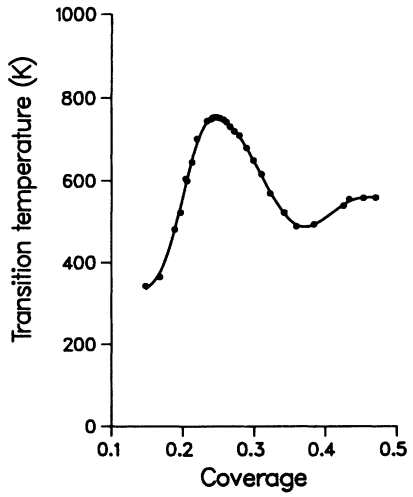

FIG. 1. Order-disorder phase boundary as determined by LEED for the O/Ru(001) system.

age is increased. The absence of these two structures in the O/Ru case is reflected in the effective Hamiltonian used in Sec. III to describe the adatom ordering observed here.

III. THEORETICAL

A. Models

We attempt to understand the interactions driving the ordering of oxygen on the ruthenium(001) surface in terms of lattice-gas models. Submonolayer ordering of chemisorbed atoms has been frequently interpreted by using such models, with a phenomenological interaction Hamiltonian describing interactions within the adsorbate.[2] The oxygen-ruthenium system studied here should be well described in a lattice-gas picture, because the strong oxygen-ruthenium bonding localizes adsorption, at least predominantly at sites of (nearly) hcp-hollow type. This has been determined by LEED (I-V and VLEED) structural studies.[19,20,22] Cluster calculations[26] predict that the adsorption bond will be weaker by 0.8 and 1.2 eV on bridge and on-top sites respectively, suggesting an energy barrier to diffusion between hollow sites of approximately this size. The transition states in the thermal diffusion process are thus insignificantly occupied, and are therefore not observed experimentally.

In the first model considered, oxygen atoms are restricted to a triangle lattice of hcp-type hollow sites, since LEED structural studies do not detect a significant population of another site type. Nevertheless, in a second model, we allow atoms to occupy both the hcp and fcc types of hollow sites, anticipating that a small spillover of atoms onto fcc-type hollow sites could alter the phase diagram significantly. This gives a honeycomb lattice of adsorption sites, with different binding energies for the two types of sites. Since the many-body energy surface describing the motion of oxgyen atoms at a Ru(001) surface is not known, we will approximate it in terms of effective, pairwise interactions within the adsorbate.

Restricting the atoms to the triangle lattice of hcp-type hollow sites, the Hamiltonian[9] is

$$H = E_1 \sum_{\langle ij \rangle_1} n_i n_j + E_2 \sum_{\langle ij \rangle_2} n_i n_j + E_3 \sum_{\langle ij \rangle_3} n_i n_j \ , \qquad (1)$$

including pairwise interaction energies E_m between the mth neighbors $\langle ij \rangle_m$, where $m = 1,2,3$ for first-, second-, and third-nearest neighbors, as shown in Fig. 2.

In the second theoretical model considered, we allow oxygen adsorption at both hcp- and fcc-type hollow sites (O/Ni) by explicitly including a small difference in binding energy F between these two sites.[26] The phenomenological Hamiltonian

$$H = E_0 \sum_{\langle ij \rangle_1} n_i n_j + E_1 \sum_{\langle ij \rangle_3} n_i n_j + E_1' \sum_{\langle ij \rangle_3} n_i n_j + E_2' \sum_{\langle ij \rangle_4} n_i n_j + E_2 \sum_{\langle ij \rangle_5} n_i n_j + F \sum_i{}' n_i \qquad (2)$$

includes pairwise interactions up to fifth neighbors on the honeycomb lattice of hollow sites, as depicted in Fig. 2.

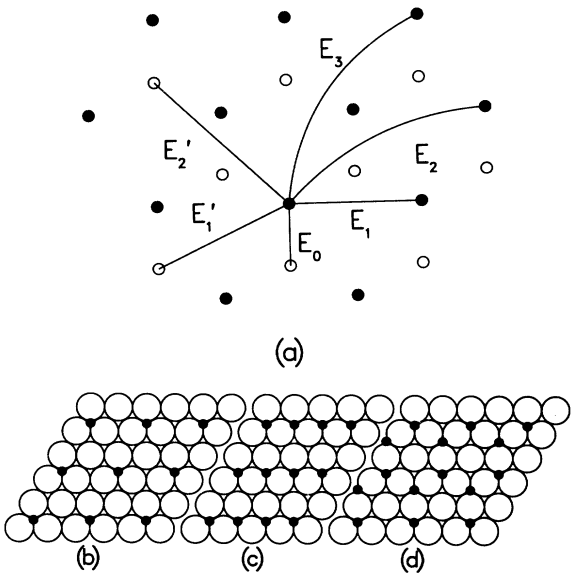

FIG. 2. Lattice-gas models. (a) The interaction energies between the first six nearest neighbors are shown. Numerical values for the energies are given in the text. Filled and open circles represent the two types of hollow sites. (b)–(d) Ordered ground states: $p(2\times2)$ at $\theta=\frac{1}{4}$, $p(2\times1)$ and (2×2) honeycomb at $\theta=\frac{1}{2}$, respectively.

Simultaneous occupation of nearest-neighbor hollow sites on the honeycomb lattice, which are separated by only 1.6 Å, is suppressed, effectively setting $E_0=\infty$. The interaction energies with second and fifth neighbors are labeled E_1 and E_2, respectively, because they correspond to first and second neighbors on a single triangle lattice; E_1 and E_2 have identical meaning in Eqs. (1) and (2). The third and fourth neighbors on the honeycomb lattice involve pairs of atoms on different site types, and have interaction energies E_1' and E_2', respectively. In the final term in Eq. (2), the primed sum runs over all sites on the triangular (sub)lattice of the less-favored adsorption site. This type of Hamiltonian has been studied previously by Roelofs *et al.*,[9] applied to the O/Ni(111) system.

The thermodynamics of these lattice-gas systems is calculated numerically by standard (Metropolis) Monte Carlo methods.[27] Simulations using Eq. (1) on the triangular lattice were performed at constant coverage employing single-particle hopping, i.e., Kawasaki-type kinetics, while the hexagonal lattice simulations based on Eq. (2) used Glauber-type kinetics in which the chemical potential is fixed, for computational reasons. (The chemical potential is chosen to obtain the desired mean coverage.) We use an order parameter ψ which is nonzero for either $p(2\times2)$ or $p(2\times1)$ order, as employed previously by Glosli and Plischke.[8] The triangular lattice may be decomposed into four triangular 2×2 sublattices. Defining the population on the pth 2×2 sublattice by N_p $(p=1,2,3,4)$, the order parameter is

$$\psi = \frac{1}{\sqrt{3}N}(\psi_1^2+\psi_2^2+\psi_3^2)^{1/2} \ , \qquad (3)$$

where

$$\psi_1 = N_1 + N_2 - N_3 - N_4 ,$$

$$\psi_2 = N_1 - N_2 + N_3 - N_4 ,$$

$$\psi_3 = N_1 - N_2 - N_3 + N_4 ,$$

and $N = N_1 + N_2 + N_3 + N_4$ is the total number of adsorbed atoms present. Notice that ψ is in fact proportional to the intensity of a $\frac{1}{2}$-order diffraction spot in the Born approximation, provided one assumes in the 2×1 case that domains orient in the three symmetry directions with equal probability. The diffraction intensities observed experimentally at normal incidence are in fact equal in all symmetry-related directions, supporting this assumption.

A susceptibility χ, derived from the fluctuations in the order parameter as

$$kT\chi = N(\langle \psi^2 \rangle - \langle \psi \rangle^2) \tag{4}$$

peaks at the order-disorder transitions studied. To distinguish between 2×2 and 2×1 ordering, we calculate a function ψ' of the order parameter ψ_α, which is nonzero only for 2×2 order, as

$$\psi' = \frac{1}{N}(\psi_1^2\psi_2^2\psi_3^2)^{1/6} . \tag{5}$$

Finally, we also compute the internal energy $E = \langle H \rangle$ and the heat capacity.

In the honeycomb lattice case, we use the same order parameter ψ defined in Eq. (3), now calculated separately for the triangular lattice of each site type. To check for $p(2\times2)$-honeycomb ordering on the honeycomb lattice, an additional order parameter ψ_H is defined as

$$\psi_H = \frac{4(N_1N_3' + N_3N_1' + N_2N_4' + N_4N_2')^{1/2}}{\sum_{i=1}^{4}(N_i + N_i')} - 1 , \tag{6}$$

where N_p' is the population of the pth 2×2 sublattice on the second (higher energy) threefold site type. It is noted that the order parameters defined here do not go precisely to zero as the order to disorder transition is crossed, due to the finite size of the system. In all cases, we define the transition temperature at a given coverage by the inflection point in the calculated graph of order parameter ψ versus temperature, as discussed further in Sec. III B.

Simulations based on Eq. (1) used a triangle lattice of size 96×96 sites, with cyclic boundary conditions, and 5000 to 200 000 Monte Carlo steps (MCS) were run per (T,Θ) point. The honeycomb lattice simulations employed a lattice of 77×77 sites with free boundary conditions to determine the phase diagram and a maximum lattice size of 153×153 in the simulations at $\Theta=\frac{1}{2}$ to determine the critical exponents. The latter simulations employed 100 000 to 700 000 MCS per data point. (The finite-size scaling results were derived from simulations on smaller lattices as well.)

B. Results and discussion

1. *Triangular lattice model*

With oxygen adsorption restricted to the triangular lattice of hcp hollow sites, ordering is governed by the Hamiltonian in Eq. (1). Repulsive interactions between first- and second-nearest neighbors (i.e., $E_1, E_2 > 0$) have been shown previously to lead to $p(2\times2)$ and $p(2\times1)$ phases near coverages of $\frac{1}{4}$ and $\frac{1}{2}$, respectively.[8] Furthermore, to suppress the formation of a $(\sqrt{3}\times\sqrt{3})R30°$ ordered phase at coverages near $\frac{1}{3}$, the second-neighbor interaction must be sufficiently strong. Ground-state arguments require that $E_2/E_1 > 0.2$ to ensure this.[28] In practice, we take $E_1 > 0$ and express all other energies in units of E_1. The magnitude of E_1 is later chosen to match the overall temperature scale of the theory to that of the experiment.

Setting $E_2 = 0.3E_1$ and $E_3 = 0$ in Eq. (1) and computing the order parameter as a function of temperature and coverage leads to the theoretical phase diagram shown in Fig. 3. The ratio E_2/E_1 was chosen so that the ratio of the order-disorder transition temperatures at coverages $\Theta = 0.25$ and 0.4 agrees roughly with that of the experiment. Choosing $E_1 = 0.23$ eV then fits the absolute transition temperatures to that of the experiment. While the actual energies of interaction are not known for the O/Ru system, energies of the magnitude proposed above are indeed plausible, in view of the oxygen-ruthenium binding energy of ≈ 6 eV.[12] Notice that first- and second-neighbor repulsive interactions are sufficient to describe the experimental phase diagram in the coverage region $0.2 < \Theta < 0.4$, but that discrepancies occur for higher coverages. For values of E_2/E_1 between 0.1 and 1, the ratio of transition temperatures for coverages $\Theta = \frac{1}{2}$

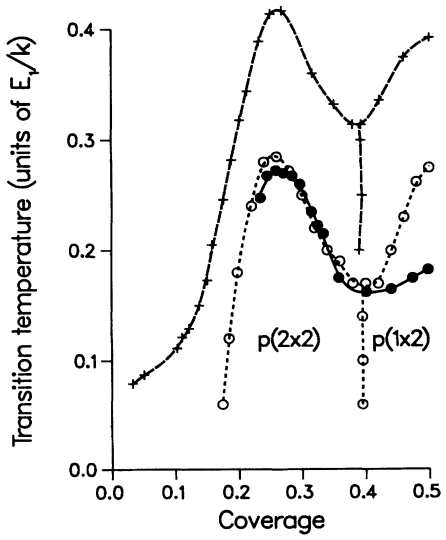

FIG. 3. Phase diagrams for lattice-gas models. (i) Open circles, triangular lattice model including first- and second-neighbor interactions $E_2 = 0.3E_1$; (ii) crosses, as above but including third-neighbor interaction $E_3 = -0.1E_1$; (iii) filled circles, honeycomb lattice-gas model, using interaction parameters listed in the text.

and $\frac{1}{4}$ is found to be in the range $0.95 < T_{1/2}/T_{1/4} < 1.06$.[8,10,28] This is in contrast to the experimental ratio of 0.74. On the other hand, apparently continuous transitions are seen at all coverages, in agreement with the experiment. In contrast, Landau theory predicts a first-order transition at $\Theta = \frac{1}{2}$ for 2×1 ordering.[21] The first-order transition may not be resolved in the simulations due to the finite size of the lattices used.[29]

The effect of an attractive interaction between third neighbors on the phase diagram is also shown in Fig. 3, for the case $E_3 = -0.1E_1$. The 2×2 and 2×1 ordered phases extend to higher temperatures, and a low-temperature phase of 2×2 islands grows in at low coverages $\Theta < \frac{1}{4}$. Although small $p(2\times2)$ islands have been seen recently by STM work[25] at room temperature, a mixed phase was not seen in our LEED measurements which were restricted to temperatures $T > 300$ K. The surface kinetics becomes too slow to ensure full thermal equilibriation at lower temperatures. We may estimate an upper limit on the magnitude of a third-neighbor attractive interaction, $|E_3| \leq 0.2E_1$, so that the island phase would be predicted to occur at temperatures lower than those of the LEED experiments.

Further contact between model and experiment is achieved by studying the critical behavior of the order-disorder transitions at coverages $\Theta = \frac{1}{4}$ and $\frac{1}{2}$, although restricting ourselves to model parameters $E_2 = 0.3E_1$ and $E_3 = 0$. The temperature dependences of the order parameter ψ, internal energy E, and susceptibility χ (see Figs. 4 and 5) are compared with the power-law scaling forms

$$E \sim E(0) \pm A_{\pm}|t|^{1-\alpha} \text{ for } t \gtrless 0 ,$$
$$\psi \sim |t|^{\beta}, \text{ and } \chi \sim |t|^{-\gamma} , \tag{7}$$

where $t = (T - T_c)/T_c$ is the reduced temperature. The transition temperature T_c may be estimated by either the peak in $\chi(T)$, or the inflection point in either $\psi(T)$ or $E(T)$, all estimates agreeing to within an accuracy of 0.2%. We have also plotted histograms of the probability distribution $P(\psi)$ for ψ, and find a double-peaked distribution in the finite-size rounded region near T_c. (This finite-size effect is present in spite of the continuous nature of the transition, and also occurs at $\Theta = \frac{1}{2}$.) The temperature at which the peaks in the $P(\psi)$ distribution corresponding to ordered and disordered phases have equal height coincides with the estimate of T_c defined above, to within the uncertainty imposed by the rounding of the transition.

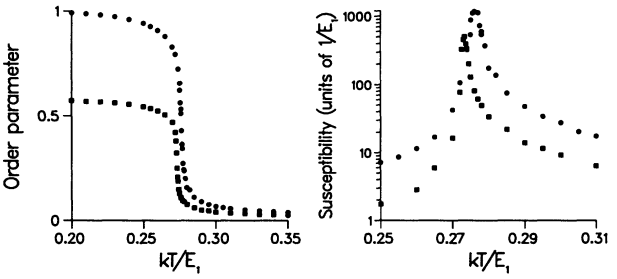

FIG. 4. Order parameter (ψ) and susceptibility (χ) calculated for the triangular lattice-gas model with first- and second-nearest-neighbor repulsive interactions. Data at coverages of $\frac{1}{4}$ and $\frac{1}{2}$ are shown by circles and squares, respectively. [By definition, ψ saturates at $1/\sqrt{3}$ for perfect $p(2\times1)$ ordering at $\Theta = \frac{1}{2}$.]

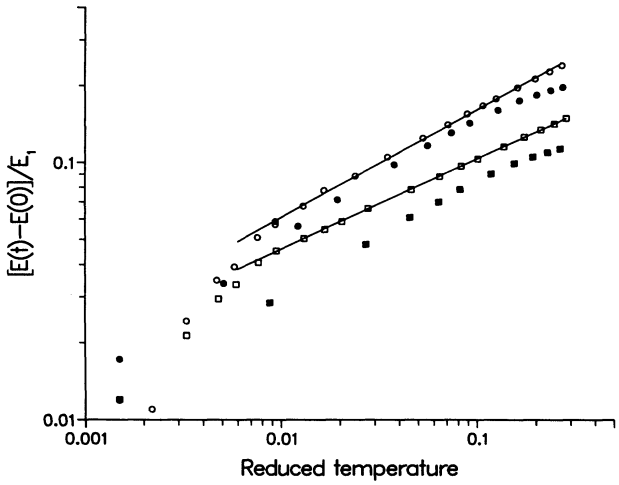

FIG. 5. Internal energy vs reduced temperature at coverages of $\frac{1}{4}$ and $\frac{1}{2}$, shown by circles and squares, respectively (using T_c estimated by finite size scaling.) Open (closed) symbols are for $T > T_c$ ($T < T_c$) cases. Solid lines give exponent fits. Statistical error bars are smaller than the symbol size for reduced temperatures $t \geq 0.01$, but the relative error in $E(T) - E(0)$ increases to 25% at $t = 0.002$.

In Fig. 5 log-log plots of the internal energy versus reduced temperature show the extent to which scaling behavior is observed; the straight lines represent the exponent determinations. In Table I the temperature regions over which scaling was observed are noted and the effective exponents α, β, and γ are listed. The exponents α and γ are determined from data at $T > T_c$; for $T < T_c$, larger deviations from power-law behavior are observed in Fig. 5, presumably due to corrections to scaling. The exponents from these simulations agree with both the experimental results and with the known values for the four-state Potts model universality class[21] to within numerical accuracy. The specific-heat exponent is somewhat less than the four-state Potts value of $\frac{2}{3}$, as was the case in previous simulations on similar models.[24] While we have thus far mimicked the experimental analysis for reasons of comparison, the exponent determination for the lattice-gas model is improved by using finite-size scaling relations[27] to extract an improved estimate for the transition temperature T_c of a (macroscopic) system. "Effective" transition temperatures $T_c(L)$ obtained in simulations at different system sizes ($L = 24$, 48, and 96) were fitted to $T_c(L) - T_c \sim L^{-1/\nu}$, giving T_c shifted by -0.35% from T_c ($L = 96$), with $\nu = 0.62 \pm 0.05$; other exponents determined using this estimate of T_c are listed in Table I. These values for α and β are closer to the exact values for the four-state Pott's model.

At a coverage $\Theta = \frac{1}{2}$, the simulations of the $p(2\times1)$

TABLE I. Effective critical exponents calculated for the triangular lattice model at coverage $\Theta=\frac{1}{4}$. The temperature range over which power-law behavior was observed depended somewhat on the exponent. The lower limit on reduced temperatures $|t|$ fitted was about 0.003–0.01, and the upper limit on $|t|$ was about 0.1–0.2. Calculated α and γ are for $T>T_c$. (T_c is given in units of E_1/k.) Experimental data for the O/Ru(001) system is also included (Ref. 6).

$T_c(L)$	α	β	γ
$T_c(96)=0.2763$	0.50±0.08	0.094±0.02	1.14±0.06
$T_c=0.2754$	0.59±0.03	0.082±0.02	1.19±0.1
Expt. O/Ru(001)	0.60±0.04	0.085±0.01	1.08±0.07

order-to-disorder transition show approximate power-law behavior leading to critical exponents that all differ significantly from the experimentally observed values, as seen in Table II. On the other hand, Fisher and Berker[30] have deduced the effective exponents $\alpha=1$, $\beta=0$, $\gamma=1$, and $\nu=\frac{1}{2}$ for scaling behavior at a first-order transition in two dimensions. Using the finite-system transition temperature defined as discussed above, our simulation result for γ is close to unity, but the other exponents differ significantly from the values given above. (Applying finite-size scaling to improve the estimate of T_c used in the exponent determination reduces β slightly.) These discrepancies may be attributed to the numerical difficulty in analyzing a weakly first transition using a model system of finite size.[29]

Although a detailed understanding of the critical behavior of this model at coverage $\Theta=\frac{1}{2}$ is at present lacking, it is nevertheless clear that the triangular lattice model is inadequate to describe the O/Ru(001) system at coverages $\Theta>0.4$. In comparison with experiment, the simulated transition based on Eq. (1) is too sharp, and occurs at too high temperatures, at $\Theta=\frac{1}{2}$. We note in passing that Glosli and Plischke[8] found a distinctly first-order transition for the 2×1 structure at $\Theta=\frac{1}{2}$, performing simulations on the same model Hamiltonian [Eq. (1)] but with $E_2/E_1=0.1$. The dependence of this nonuniversal behavior on the interaction parameter E_2/E_1 is not considered further here.

2. *Honeycomb lattice model*

In fitting the triangular lattice model to the O/Ru phase diagram, a nearest-neighbor repulsive interaction $E_1=0.23$ eV was required. The binding-energy difference F of an oxygen atom between hcp and fcc hollow sites could also be of this order of magnitude.[26] The honeycomb lattice model defined in Sec. III A explicitly includes the occupation of both site types, as may be expected to occur in this situation to some degree. This model reduces to the triangular lattice model in the limit of sufficiently large difference F in binding energy, forcing all the atoms back onto the lower energy sites. The ordered structure at coverage $\Theta=\frac{1}{2}$ is then $p(2\times1)$. On the other hand, at low enough values of F, the 2×2-honeycomb structure may form at $\Theta=\frac{1}{2}$, instead of the $p(2\times1)$; see Fig. 2(d). Two sets of interaction parameters were considered, both giving $p(2\times2)$ ordering at $\Theta=\frac{1}{4}$. Taking $E_1'=E_1$ and $E_2'=E_2=0.3E_1$ favors 2×1 ordering instead of the honeycomb structure at $\Theta=\frac{1}{2}$, for all values of F. The 2×1 structure forms on the favored triangular sublattice. However, the phase diagram for this model predicts order-disorder transition temperatures of similar magnitudes at coverages $\frac{1}{4}$ and $\frac{1}{2}$, in disagreement with the experiment. This parameter set is not considered further, as it does not appear to help in understanding the oxygen-ruthenium system considered here.

As a second parameter choice, we set $E_2=E_1'=0.3E_1$ and $E_2'=0$. The important difference here is the reduction of E_1' relative to E_1, allowing the existence of a 2×2-honeycomb structure at sufficiently low values of F. The ground-state energies of the 2×1 and honeycomb structures are in this case degenerate at $F=1.7E_1$. (Compared to the lattice gas models of Roelofs *et al.*[9] and Bartelt, Einstein, and Roelofs[31] for the O/Ni(111) system, the lack of a $(\sqrt{3}\times\sqrt{3})R30°$ structure in the O/Ru(001) data requires the much larger value of the repulsive interaction E_2 here.)

Occupation of the unfavored site type generally increases as F decreases, although this effect is in fact strongly coverage dependent. Simulations show that for the parameters listed above, less than 0.5% of the adsorbed atoms reside on the higher-energy site type, at coverage $\Theta=\frac{1}{4}$, and the $p(2\times2)$ order-to-disorder transi-

TABLE II. Effective critical exponents at coverage $\Theta=\frac{1}{2}$, calculated for the triangular and honeycomb lattice models. Values of T_c are in units of E_1/k. Experimental data also included from Ref. 7.

$T_c(L)$	α	β	γ
Triangular lattice			
$T_c(96)=0.2733$	0.54±0.05	0.079±0.02	0.97±0.04
$T_c=0.2724$	0.64±0.03	0.063±0.006	1.06±0.06
Honeycomb lattice			
$T_c=0.1729$		0.066±0.015	1.15±0.14
Expt. O/Ru(001)	0.30±0.06	0.13±0.02	1.35±0.15

tion temperature at this coverage is only slightly decreased, in comparison to the triangular lattice model, as shown in Fig. 3. In contrast, the $p(2\times1)$ phase at $\Theta=\frac{1}{2}$ disorders at a significantly reduced temperature $T_{1/2}$. For $F=2.2E_1$, $T_{1/2}/T_{1/4}=0.74$, very close to that found experimentally. This decrease in $T_{1/2}$ is accompanied by an increase in the relative occupation of the higher-energy adsorption site type, as shown in Fig. 6 as a function of coverage. At a coverage of $\Theta=\frac{1}{2}$, the percentage of adatoms that spill over onto the second site type is 3% at temperatures slightly below $T_{1/2}$ and 12% just above $T_{1/2}$, compared to the value of 10% at $T_{1/2}$, which is that plotted in Fig. 6. As F decreases, the transition at $\Theta=\frac{1}{2}$ broadens, becoming almost obscured in the vicinity of $F=1.7E_1$ due to competition between (2×1) and honeycomb-ordered structures. For lower values of F, the (2×2) honeycomb structure forms as the low-temperature ordered phase.

In Fig. 3 the order-disorder phase boundary calculated on the honeycomb lattice model with $F=2.2E_1$ is found to be very similar to that of the O/Ru experiment (see Fig. 1.), at all experimentally attainable coverages—i.e., $\Theta\leq\frac{1}{2}$. The strong $p(2\times2)$ phase occurring near $\Theta=\frac{1}{4}$ gives way to a $p(2\times1)$ phase near $\Theta=\frac{1}{2}$ that is weakened by the spill over of atoms onto the second hollow site type. The minimum in the order-disorder transition temperature at $\Theta=0.4$ accompanies the transition between 2×2 and 2×1 ordered phases. Note that the slight shift in the peak transition temperature from $\Theta=0.25$ to 0.26 in the honeycomb lattice simulations is due mainly to the use of free boundary conditions, and is a finite-size artifact that is of no concern here. These simulations used a lattice of 77×77 sites. [A very minor contribution to this shift in optimal coverage may arise from the extremely small spillover of adatoms onto the second site type. This latter effect is NOT a theoretical artifact. If this spillover were significantly larger at $\Theta=\frac{1}{4}$, our experimental fine tuning of the calibration of the coverage would be in error, because it is based on the point at which $p(2\times2)$ ordering is optimal.] In the simulations described below, it was found that the observed transition behavior, at coverages shifted slightly from those quoted, is only slightly altered.

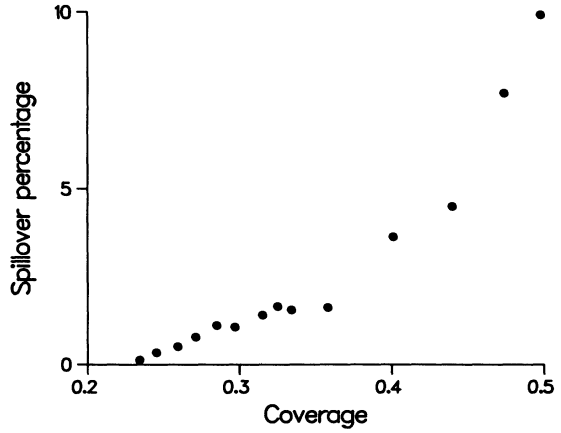

FIG. 6. Percentage of adatoms occupying the higher-energy adsorption-site type, as a function of total coverage. The energy difference between the two types of hollow sites is $F=2.2E_1$, and the spillover is calculated at the order-disorder transition temperature.

Critical exponents are calculated at $\Theta=\frac{1}{2}$ for this honeycomb lattice model, and listed in Table II. When at first the finite-system transition temperature $T_c=0.1755E_1$ is used in determining the effective exponents, fitted values for γ_+ and γ_- differ considerably from one another, with $\gamma_+\approx0.83$ unphysically low and $\gamma_-\approx2.88$ unphysically high. By adjusting T_c, it is found that for $T_c=0.172\,90E_1$, the exponent fits give $\gamma_-=\gamma_+$. If the finite-size scaling of $T_c(L)$ is fitted using T_c given above, we obtain an estimate of $\nu=0.65\pm0.01$. The values of β,γ (see Table II), and ν determined in this way are very close to the four-state Pott's model values, as will be discussed shortly, and are shifted somewhat away from those obtained in the triangular lattice-gas simulations described previously.

Landau rules predict that the $p(2\times1)$ disordering transition is first order on triangular and honeycomb lattices. It appears that our simulations are not describing this asymptotic region, which is presumably masked by finite-size effects. On the other hand, the set of interaction parameters chosen here is near the crossover between the honeycomb and (2×1) ground states at $\Theta=\frac{1}{2}$. Noting that a (2×2)-honeycomb order-disorder transition is in the four-state Pott's class,[21] it is plausible that the simulation data is outside the critical region for the $p(2\times1)$-to-disorder transition and that the effective exponents of the simulations are influenced by a crossover to four-state Pott's-model behavior. Our ability to probe further into the asymptotic region is limited by finite-size effects in the simulations.

The effective exponents of the honeycomb lattice-gas model do not agree well with those measured experimentally for the O/Ru system, although the exponent γ is shifted in the direction of the experimental value, when compared to the result for the triangular lattice-gas model, as seen in Table II. Besides the crossover phenomena suggested above, the critical behavior could be masked experimentally by other effects. Deliberately introduced steps on the Ru(001) surface have been shown to dramatically alter the observable critical behavior of oxygen ordering at the lower coverage of $\frac{1}{4}$.[32] At coverage $\Theta=\frac{1}{2}$, 2×1 domains with rows of oxygen atoms oriented parallel to the steps were suppressed in measurements on a Ru[17(001)×(100)] crystal.[17] It should also be noted that the effect of the observed reconstruction at $\Theta=\frac{1}{2}$ may not be adequately described in the lattice-gas models used here, and could thus alter the magnitude of corrections to scaling behavior. We note finally that, although the experimental determination of T_c from the inflection point of the order parameter (or alternatively from the integrated LEED spot intensity) is made on a finite system, the power-law fits to the experiment were not improved overall by adjusting T_c further.

We note in passing that the degree of rounding of the transition at $\Theta=\frac{1}{2}$ due to finite-system size in the honeycomb lattice-gas model is similar to that observed experi-

mentally, while the simulations of the triangle lattice model show less rounding, for a similar size of system. Of course, the (different) boundary conditions used in the two models are not meant to simulate those of the O/Ru system in even a qualitative way.

IV. SUMMARY

The comprehensive set of LEED studies[6,7,19,20,22] on the structural properties of the O/Ru(001) system led us to investigate lattice-gas models as candidates for describing the observed phase diagram and critical behavior. The single-phase $p(2\times2)$ ordered phase observed at coverages near $\Theta=\frac{1}{4}$ can be well understood in terms of a triangle lattice model that simulates adsorption on a single type of threefold hollow site only. Relatively strong first- and second-nearest-neighbor repulsive interactions ($E_1=0.23$ eV, $E_2=0.3E_1$) between adsorbed atoms are sufficiently to describe the sharp peak in the $(T-\Theta)$ phase boundary, and the lack of a $(\sqrt{3}\times\sqrt{3})R30°$ phase. The appearance of cluster formation[25] only at low coverages and at temperatures below about 300 K places an approximate upper limit on an effective third-nearest-neighbor attractive interaction of $|E_3|\leq 0.046$ eV.

However, the triangular lattice model predicts an order-disorder transition temperature at $\Theta=\frac{1}{2}$ that is much larger than that of the O/Ru system, in relation to the transition at $\frac{1}{4}$ coverage. In a honeycomb lattice model, adsorption on both hcp- and fcc-type hollow sites is permitted. Choosing binding energies for these two site types differing by $F=0.52$ eV, the transition temperature at coverages above $\Theta\approx 0.4$ are reduced markedly, in much better agreement with the O/Ru phase diagram. This behavior is accompanied by a small spillover of 3–10 % of the adatoms onto the higher-energy site type, at coverages from 0.4 to 0.5, at the corresponding transition temperatures. Since the spillover becomes negligible at lower coverages, the effect on the $p(2\times2)$ phase near $\Theta=\frac{1}{4}$ is minimal. Effective exponents at the $\Theta=\frac{1}{2}$ transition are found to differ somewhat, comparing the triangle-lattice gas ($F=\infty$) and honeycomb lattice ($F=2.2E_1$) simulations. In the latter case, the calculated effective exponents agree well with those of the four-state Pott's model, suggestive of crossover behavior between the $p(2\times1)$ and $p(2\times2)$-honeycomb ordered states. The poor agreement of the exponents of either model with those measured for the O/Ru system at $\Theta=\frac{1}{2}$ may be due to nonuniversal corrections to scaling or boundary effects, for which the two models may lack sufficiently accurate Hamiltonians. The measured exponents are in fact close to those of a three-state Pott's model. However, we have been unable to find any reasonable explanation for a reduction in symmetry of the lattice-gas model of the oxygen on ruthenium system that would account for this behavior.

Nevertheless, it has been demonstrated, using lattice-gas models, that a relatively small population of adatoms on a higher-energy adsorption site may affect adsorbate-ordering properties markedly, as seen most clearly in this case in the phase diagram. Order-disorder transition behavior in the O/Ru(001) system have been presented and interpreted as a candidate for which such a spillover effect may be important.

ACKNOWLEDGMENTS

This work was supported by the Deutsche Forschungsgemeinschaft (Sonderforschungsbereich 128 and 338), and by the Natural Sciences and Engineering Research Council of Canada.

*Permanent address: Physics Department, Trent University, Peterborough, Ontario, Canada K9J 7B8.

[1] *Order in Two Dimensions,* edited by S. Sinha (North-Holland, New York, 1980); E. Bauer, in *Structure and Dynamics of Surfaces II,* edited by W. Schommers and P. von Blanckenhagen (Springer-Verlag, Berlin, 1987), p. 115.

[2] T. L. Einstein, in *Proceedings of the Tenth John Hopkins Workshop: Infinite Lee Algebras and Conformal Invariance in Condensed Matter and Particle Physics,* edited by K. Dietz and V. Ritterberg (World Scientific, Singapore, 1987), p. 17.

[3] T. E. Felter, S. M. Foiles, M. S. Daw, and R. H. Stulen, Surf. Sci. **171**, L379 (1986); J.-P. Muscat, Phys. Rev. B **33**, 8136 (1986); T. L. Einstein, M. S. Daw, and S. M. Foiles, Surf. Sci. **227**, 114 (1990).

[4] T. L. Einstein, in *Chemisry and Physics of Solid Surfaces VII,* edited by R. Vanselow and R. F. Howe (Springer, Berlin, 1988), p. 307.

[5] P. Piercy, M. Maier, and H. Pfnür, in *Three Structure of Surfaces II,* edited by J. F. van der Veen and M. A. Van Hove (Springer-Verlag, Berlin, 1988), p. 480.

[6] H. Pfnür and P. Piercy, Phys. Rev. B **40**, 2515 (1989).

[7] H. Pfnür and P. Piercy, Phys. Rev. B **41**, 582 (1990).

[8] J. Glosli and M. Plischke, Can. J. Phys. **61**, 1515 (1983).

[9] L. D. Roelofs, A. R. Kortan, T. L. Einstein, and R. L. Park, J. Vac. Sci. Technol. **18**, 492 (1981); L. D. Roelofs, in *Chemistry and Physics of Solid Surfaces IV,* edited by R. Vanselow and R. Howe (Springer-Verlag, Berlin, 1982), p. 219.

[10] K. De'Bell, H. Pfnür, and P. Piercy, in *The Structure of Surfaces III,* edited by S. Y. Tong, M. A. Van Hove, K. Takayanagi, and Xie Xide (Springer, Berlin, 1991).

[11] R. L. Park, T. L. Einstein, A. R. Kortan, and L. D. Roelofs, in *Order in Two Dimensions,* edited by S. Sinha (North-Holland, New York, 1980), p. 17.

[12] T. E. Madey, H. A. Engelhardt, and D. Menzel, Surf. Sci. **48**, 304 (1975).

[13] J. C. Fuggle, T. E. Madey, M. Steinkilberg, and D. Menzel, Surf. Sci. **52**, 521 (1975).

[14] G. E. Thomas and W. H. Weinberg, J Chem. Phys. **70**, 954 (1979).

[15] T. S. Rahman, A. B. Anton, N. R. Avery, and W. H. Weinberg, Phys. Rev. Lett. **51**, 1979 (1983).

[16] H. I. Lee, G. Praline, and J. M. White, Surf. Sci. **91**, 581 (1980); S. K. Shi and J. M. White, J. Chem. Phys. **73**, 5889 (1980).

[17] L. Parrot, G. Praline, B. E. Koel, J. M. White, and T. N. Taylor, J. Chem. Phys. **71**, 3352 (1979).

[18]L. Surnev, G. Rangelov, and G. Bliznakov, Surf. Sci. **159**, 229 (1985).
[19]M. Lindoos, H. Pfnür, G. Held, and D. Menzel, Surf. Sci. **222**, 451 (1989).
[20]H. Pfnür, G. Held, M. Lindroos, and D. Menzel, Surf. Sci. **220**, 43 (1989).
[21]M. Schick, Prog. Surf. Sci. **11**, 245 (1981).
[22]H. Pfnür, M. Lindroos, and D. Menzel, Surf. Sci. **248**, 1 (1991).
[23]M. Maier, Diplomarbeit, Technische Universität München, 1986 (unpublished).
[24]N. C. Bartelt, T. L. Einstein, and L. D. Roelofs, Phys. Rev. B **32**, 2993 (1985).
[25]C. Günther and R. J. Behm (unpublished).
[26]A. B. Anderson and M. K. Awad, Surf. Sci. **183**, 289 (1987).
[27]*Applications of the Monte Carlo Method in Statistical Physics*, 2nd ed., edited by K. Binder (Springer-Verlag, Berlin, 1987); *Monte Carlo Methods in Statistical Physics* (Springer, Berlin, 1979).
[28]J. S. Walker and M. Schick, Phys. Rev. B **20**, 2088 (1979).
[29]O. G. Mouritsen, *Computer Studies of Phase Transitions and Critical Phenomena* (Springer, Berlin, 1984).
[30]M. E. Fisher and A. N. Berker, Phys. Rev. B **26**, 2507 (1982).
[31]N. C. Bartelt, T. L. Einstein, and L. D. Roelofs, Phys. Rev. B **35**, 6786 (1987).
[32]M. Sokolowski and H. Pfnür, Phys. Rev. Lett. **63**, 183 (1989).